# Considerations & issues in the radius extraction

Douglas Higinbotham

Jefferson Lab

Low Q Workshop: 17 May 2023

# A Puzzle Caused By Tenacious Graduate Students

Randolf Pohl, Aldo Antognini, *et al.,* Nature **466** (2010) 213–216.

The signal was nearly not found as they had been scanning frequencies assuming a large radius.

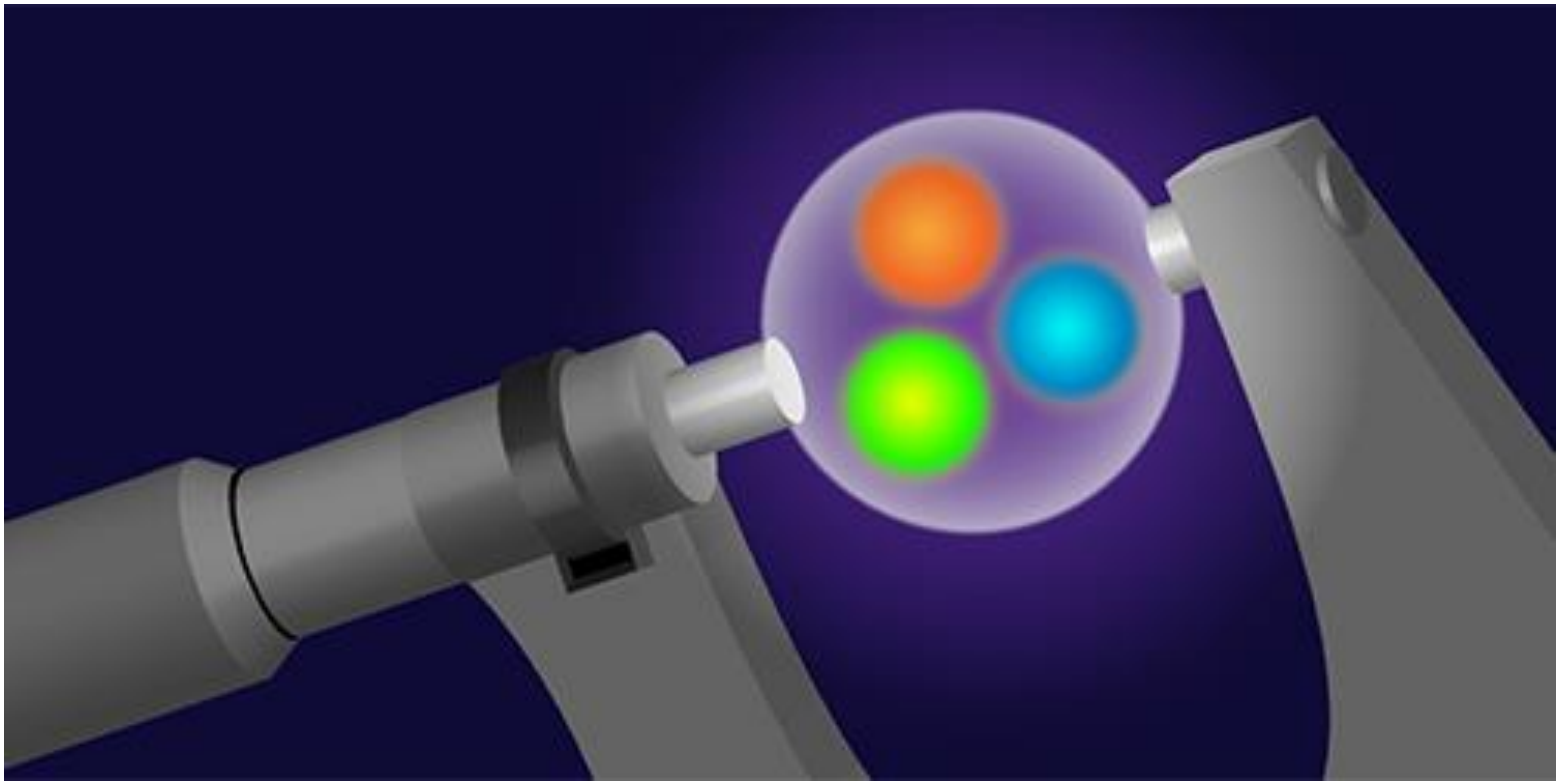

Figure by APS/Alan Stonebraker

# How do we typically do elastic electron scattering measurements?

- Beam of electrons from an accelerator (E)
- Place target material in the beam
  - Foils are easy, nearly point (typically thin) targets and thickness is easy to determine
  - Cryo-targets are challenging (e.g. boiling effects, energy loss)
  - **Since target thickness cannot be exactly determined, floating normalizations are often used.**
- For elastic measurement can measure scattered electron (E') and/or proton.
  - Over determined reaction
- Spectrometers are typically used
  - Magnetic fields, wire-chambers, reconstructed tracks, sieve data, etc.

Low Q Workshop 2023
and in Hall A 2002:
Jian-Ping Chen
Zein-Eddine Meziani
Ron Gilman
Douglas Higinbotham
Eric Voutier

# Electron Scattering Charge Radii from Nuclei

Fourier Transformation of Ideal Charge Distributions.

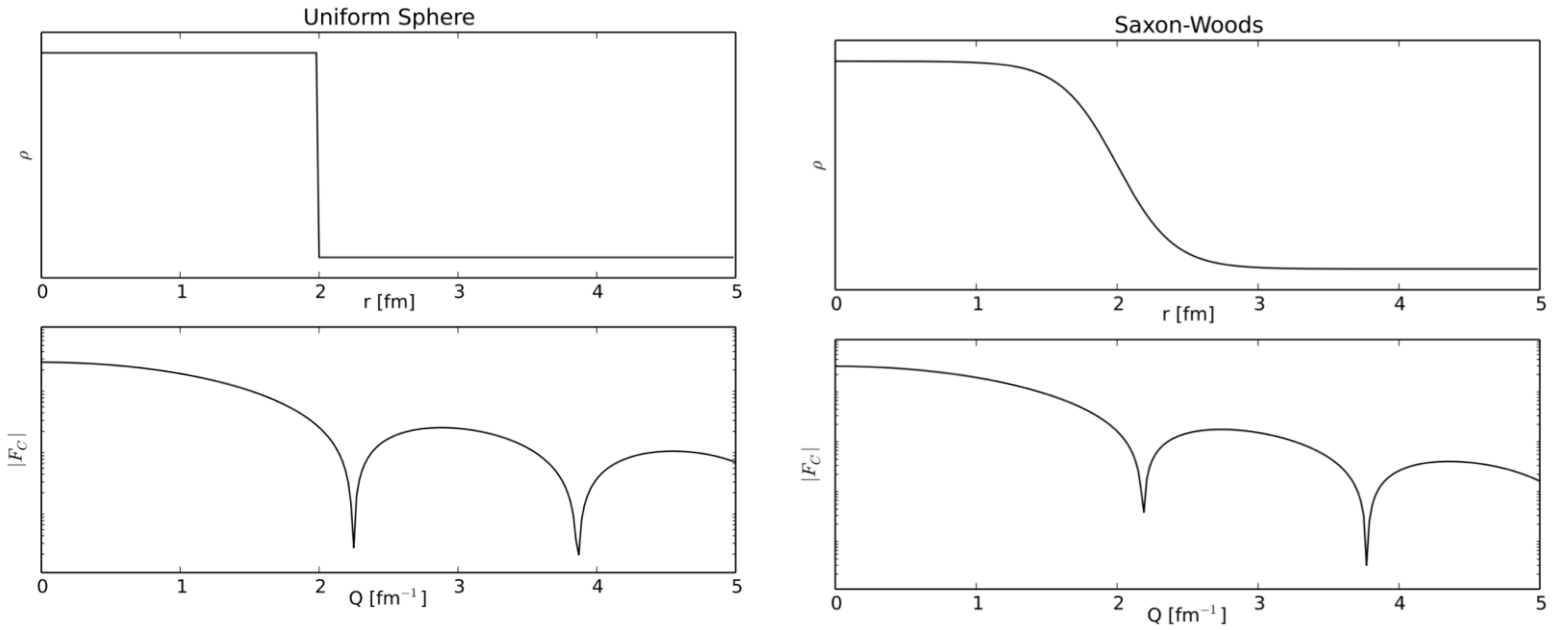


*Example Plots Made By R. Evan McClellan while Jefferson Lab Postdoc now Professor at* Pensacola State College*)*

e.g. for Carbon: Stanford high $Q^2$ data from I. Sick and J.S. McCarthy, Nucl. Phys. **A150** (1970) 631.
National Bureau of Standards low $Q^2$ data from L. Cardman *et. al*., Phys. Lett. **B91** (1980) 203.

# Determining the Charge Radius of Carbon

High $Q^2$ data from I. Sick and J.S. McCarthy, Nucl. Phys. **A150** (1970) 631.
National Bureau of Standards low $Q^2$ data from L. Cardman et. al., Phys. Lett. **B91** (1980) 203.

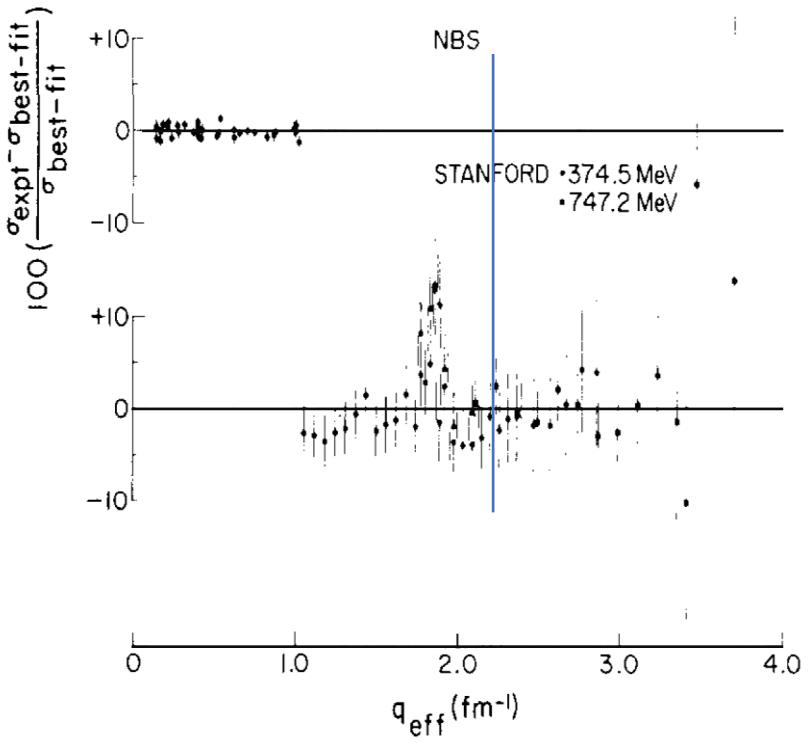


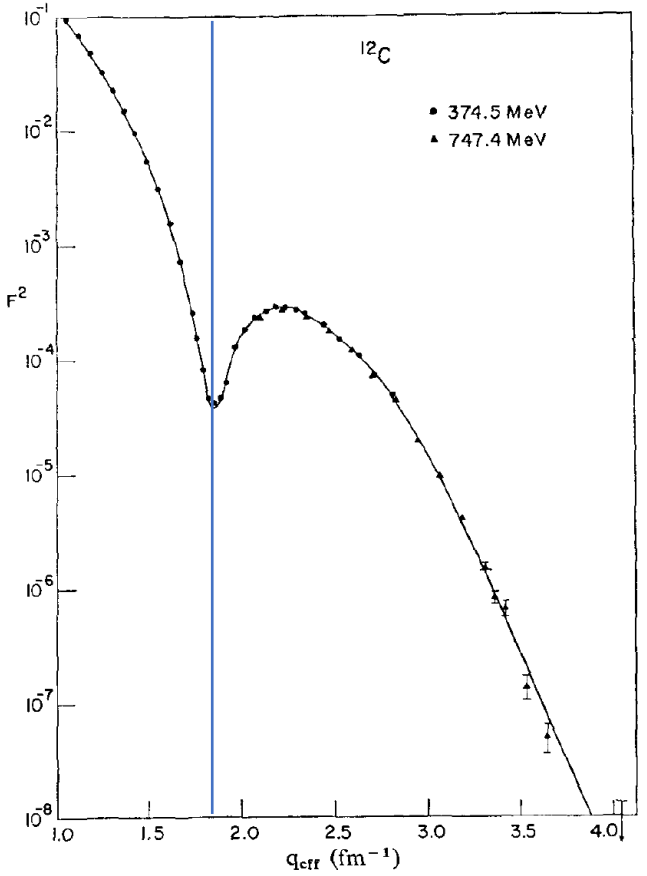


See the L. Cardman's paper for details of the carbon radius ( 2.46 fm ) analysis.

# Charge Radius of the Proton

- Proton $G_E$ has no measured minima and is far too light for the Fourier transformation to work in a model independent way.
- Thus for the proton we make use of the fact that as $Q^2$ goes to zero the charge radius is proportional to the slope of $G_E$

$$r_p \equiv \left( -6 \left. \frac{dG_E(Q^2)}{dQ^2} \right|_{Q^2=0} \right)^{1/2}$$

**This definition of $r_P$ has been shown to be consistent with the radius extracted from the muonic hydrogen data.**

M. I. Eides, H. Grotch and V. A. Shelyuto, Phys. Rept.342 (2001) 63. http://doi.org/10.1016/S0370-1573(00)00077-6
Gerald A. Miller, Phys. Rev. C **99** (2019) 035202. https://doi.org/10.1103/PhysRevC.99.035202

**As we cannot measure at exactly $Q^2$=0 this will be an extrapolation problem.**

# Elastic Electron Scattering from Spin-1/2 Particles

From relativistic quantum mechanics one can derive the formula for electron-proton scattering where one has assumed the exchange of a single virtual photon.

$$\frac{d\sigma}{d\Omega} = \left(\frac{d\sigma}{d\Omega}\right)_{\text{Mott}} \cdot \frac{E'}{E}\left[\frac{G_E^2 + \tau G_M^2}{1+\tau} + 2\tau G_M^2 \tan^2\frac{\theta}{2}\right]$$

where $G_E$ and $G_M$ form factors take into account the finite size of the proton.

$$G_E = G_E(Q^2),\ G_M = G_M(Q^2);\ \ G_E(0)=1,\ G_M(0) = \mu_p$$

$$Q^2 = 4\ E\ E'\ \sin^2(\theta/2) \text{ and } \tau = Q^2/4m_p^2$$

Elastic cross sections at small angles and small $Q^2$'s are dominated by $G_E$ ( JLab PRad Hall B )

Elastic cross sections at large angles and large $Q^2$'s are dominated by $G_M$ ( JLab GMP Hall A )

For moderate $Q^2$'s one can separate $G_E$ and $G_M$ with the Rosenbluth technique (same $Q^2$ different E,θ).

# $G_E$ and $G_M$ Contributions To The Cross Section

Plots by Ethan Buck (Jefferson Lab SULI Student and W&M undergraduate)

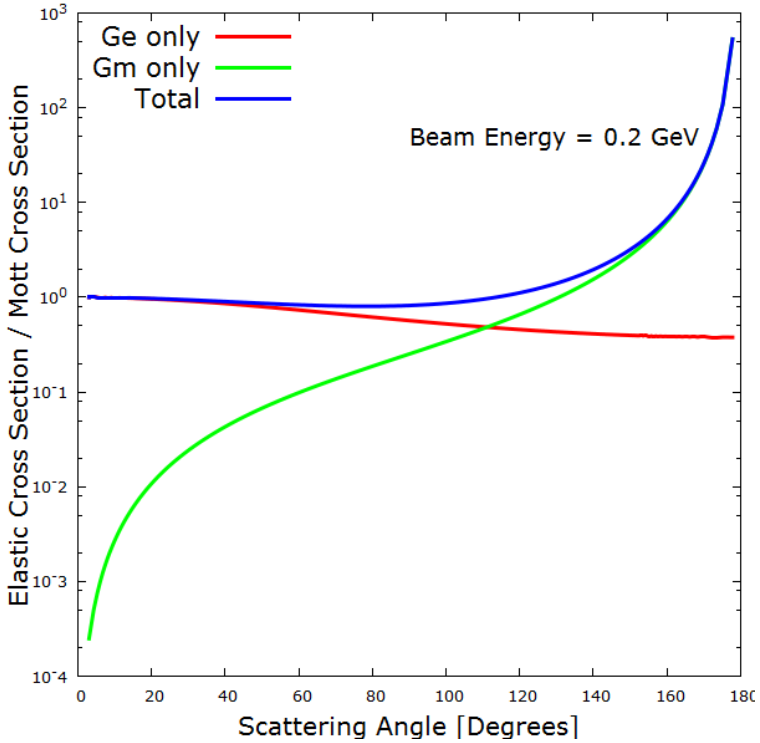


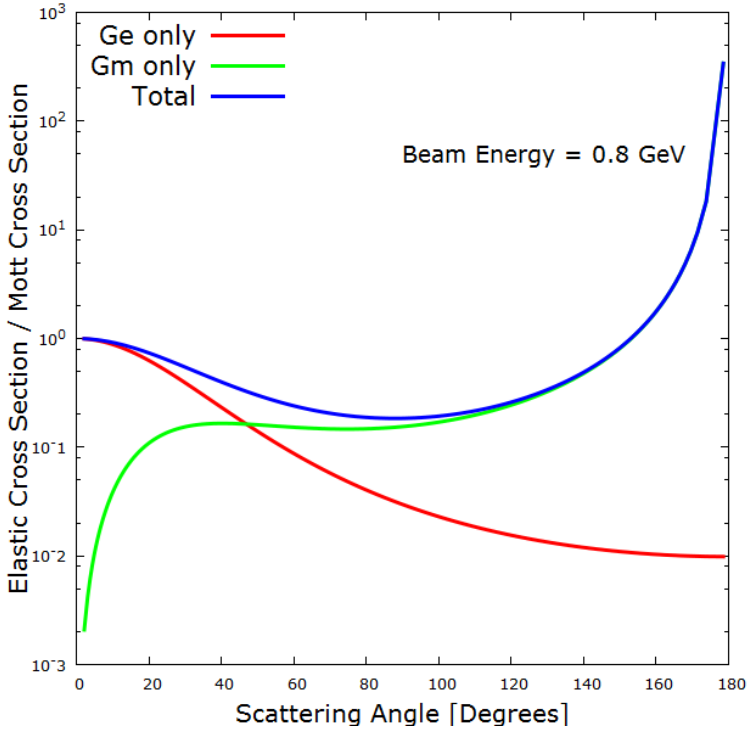


Experiments like PRad (Hall B) go to small angle to maximize $G_E$ and minimize $G_M$ contribution..

Global fits, like typically done with the Mainz 2010 data, need several normalization, $G_E$ and $G_M$

# Radii from Electron Scattering Is A Story Of Many Results

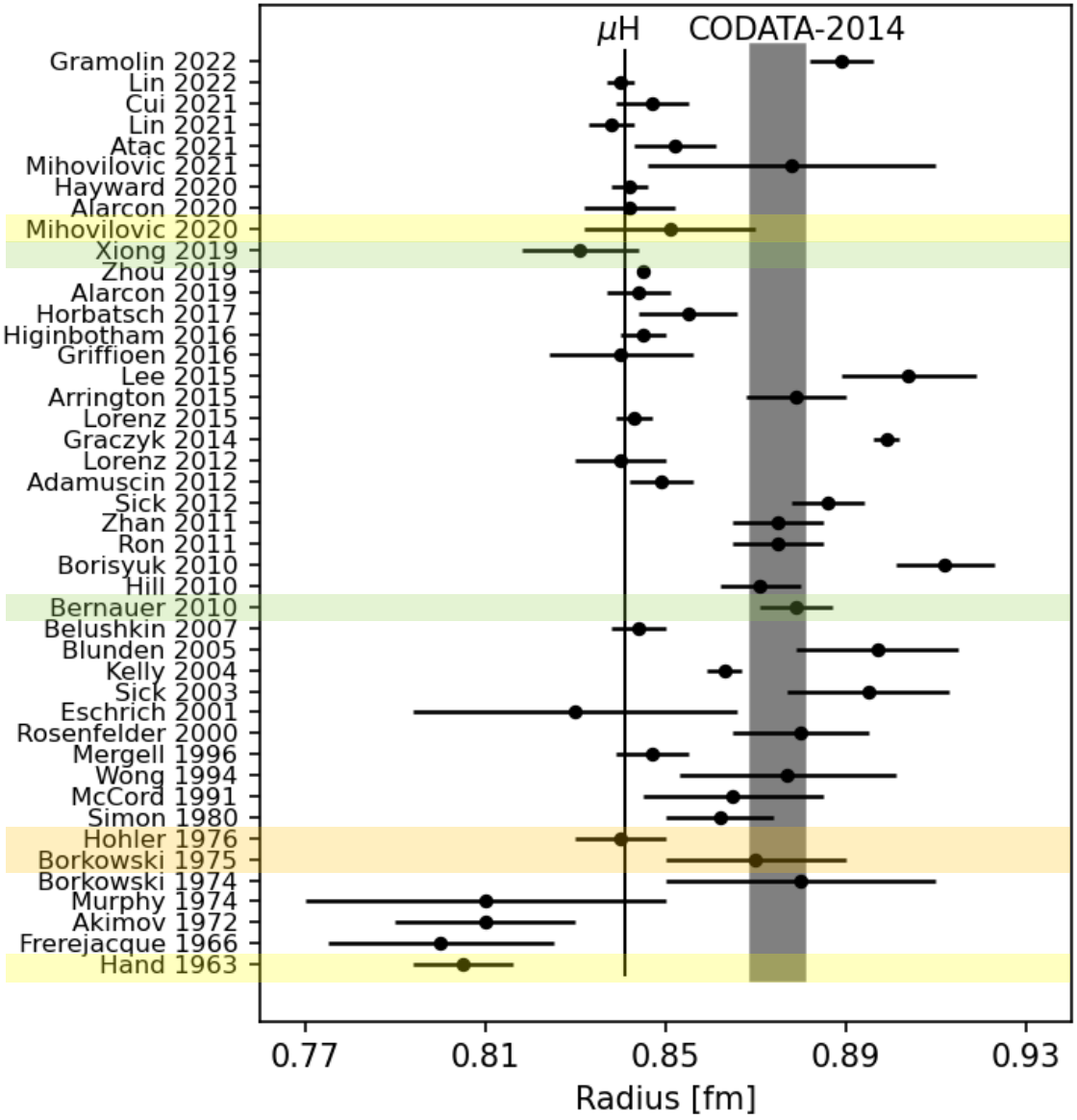



Gramolin 2022: https://doi.org/10.1103/PhysRevD.105.054004
Lin 2022: https://doi.org/10.1103/PhysRevLett.128.052002
Cui 2021: https://doi.org/10.1103/PhysRevLett.127.092001
Lin 2021: https://doi.org/10.1016/j.physletb.2021.136254
Atac 2021: https://doi.org/10.1140/epja/s10050-021-00389-9
Mihovilovic 2021: https://doi.org/10.1140/epja/s10050-021-00414-x
Hayward 2020: https://doi.org/10.1016/j.nuclphysa.2020.121767
Alarcon 2020: https://doi.org/10.1103/PhysRevC.102.035203
Mihovilovic 2020: https://doi.org/10.3389/fphy.2020.00036
Xiong 2019: https://doi.org/10.1038/s41586-019-1721-2
Zhou 2019: https://doi.org/10.1103/PhysRevC.99.055202
Alarcon 2019: https://doi.org/10.1103/PhysRevC.99.044303
Horbatsch 2017: https://doi.org/10.1103/PhysRevC.95.035203
Higinbotham 2016: https://doi.org/10.1103/PhysRevC.93.055207
Griffioen 2016: https://doi.org/10.1103/PhysRevC.93.065207
Lee 2015: https://doi.org/10.1103/PhysRevD.92.013013
Arrington 2015: https://doi.org/10.1063/1.4921430
Lorenz 2015: https://doi.org/10.1103/PhysRevD.91.014023
Graczky 2014: https://doi.org/10.1103/PhysRevC.90.054334
Lorenz 2012: https://doi.org/10.1140/epja/i2012-12151-1
Adamuscin 2012: https://doi.org/10.1016/j.ppnp.2012.01.014
Sick 2012: https://doi.org/10.1016/j.ppnp.2012.01.013
Zhan 2011: https://doi.org/10.1016/j.physletb.2011.10.002
Ron 2011: https://doi.org/10.1103/PhysRevC.84.055204
Borisyuk 2010: https://doi.org/10.1016/j.nuclphysa.2010.05.054
Hill 2010: https://doi.org/10.1103/PhysRevD.82.113005
Bernauer 2010: https://doi.org/10.1103/PhysRevLett.105.242001
Belushkin 2007: https://doi.org/10.1103/PhysRevC.75.035202
Blunden 2005: https://doi.org/10.1103/PhysRevC.72.057601
Kelly 2004: https://doi.org/10.1103/PhysRevC.70.068202
Sick 2003: https://doi.org/10.1016/j.physletb.2003.09.092
Eschrich 2001: https://doi.org/10.1016/S0370-2693(01)01285-0
Rosenfelder 2000: https://doi.org/10.1016/S0370-2693(00)00316-6
Mergell 1996: https://doi.org/10.1016/0375-9474(95)00339-8
Wong 1994: https://doi.org/10.1142/S0218301394000255
McCord 1991: https://doi.org/10.1016/0168-583X(91)96079-Z
Simon 1980: https://doi.org/10.1016/0375-9474(80)90104-9
Hohler 1976: https://doi.org/10.1016/0550-3213(76)90449-1
Borkowski 1975: https://doi.org/10.1007/BF01409496
Borkowski 1974: https://doi.org/10.1016/0550-3213(75)90514-3
Murphy 1974: https://doi.org/10.1103/PhysRevC.9.2125
Akimov 1972: http://www.jetp.ac.ru/cgi-bin/dn/e_035_04_0651.pdf
Frerejacque 1966: https://doi.org/10.1103/PhysRev.141.1308
Hand 1963: https://doi.org/10.1103/RevModPhys.35.335


CODATA 2014: Proton Radius 0.8751(61)fm and **Rydberg Constant** 10 973 731.568 508(65)$m^{-1}$

CODATA 2018: Proton Radius 0.8414(19)fm and **Rydberg Constant** 10 973 731.568 160(21)$m^{-1}$

# PRad: Hall B Proton Radius Experiment

Small angle and small $Q^2$ to minimize the effects of $G_M$ and provide best measurement of $G_E$
Gas Target (the proton), GEM Detectors (scattering angles), Calorimeter (energy & position)

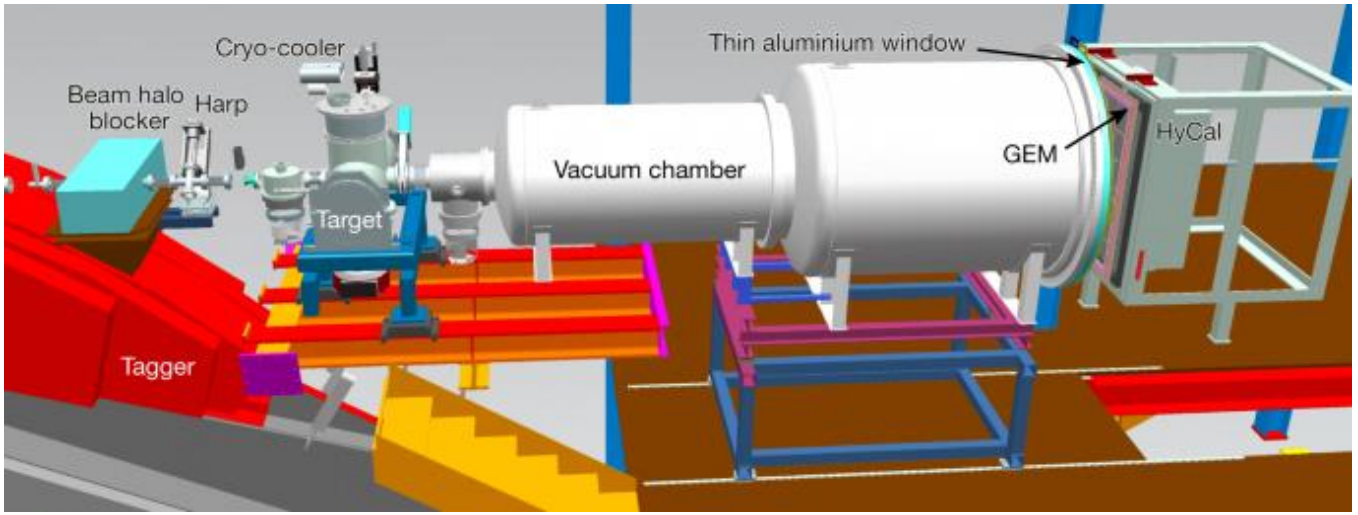

# Model Selection For PRad **BEFORE** Seeing The Data

Z. Yan, DH, *et al.*, Phys. Rev. C 98 (2018) 025204; https://doi.org/10.1103/PhysRevC.98.025204

*Shown are a subset of the results of fitting the full range of expected data with lots of different charge form factor functions and radii.*

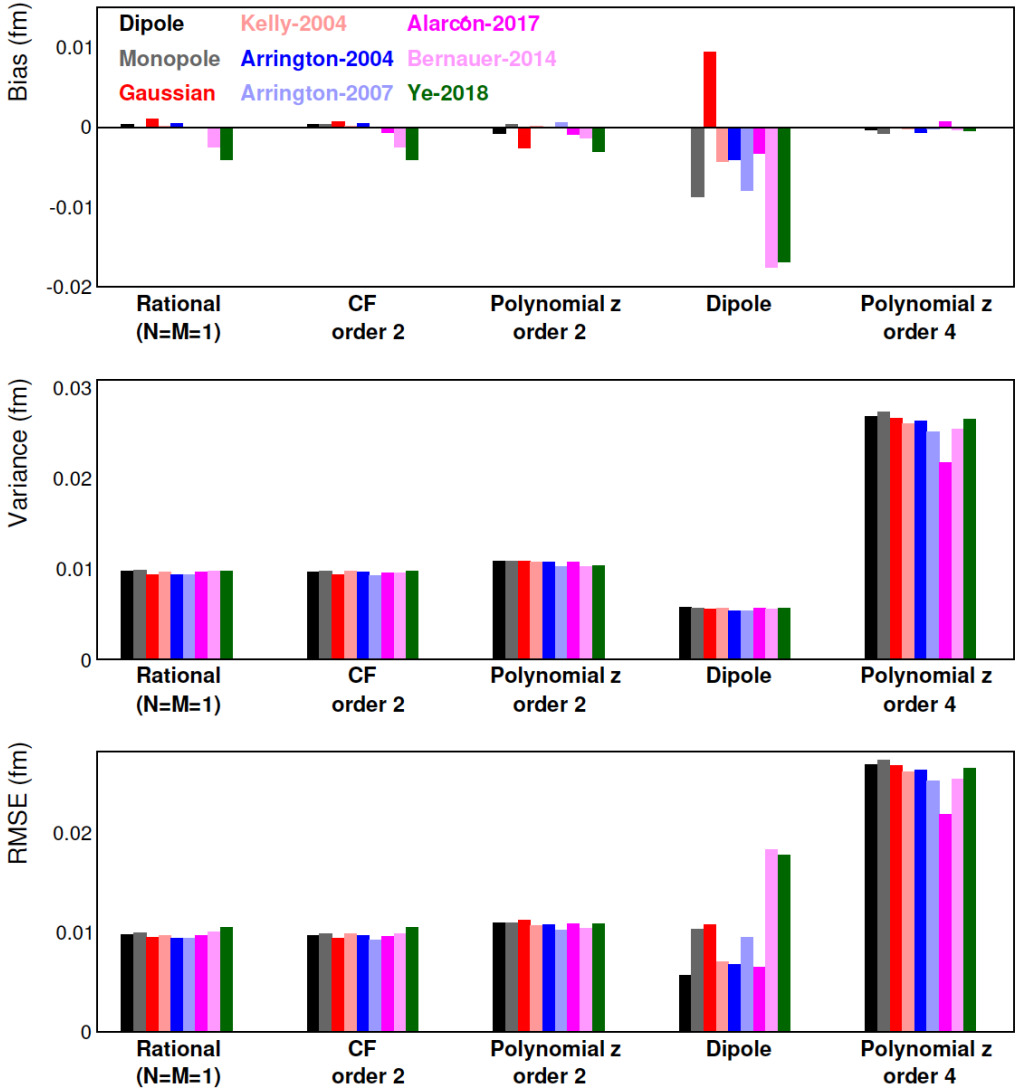


Since we know the true radius for these functions we can calculation the bias: the offset from the true value.


bias low, variance low

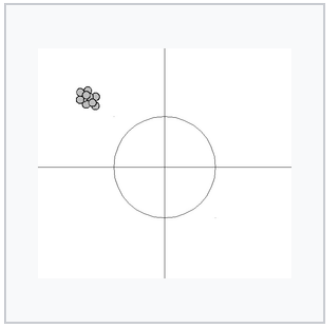

bias high, variance low

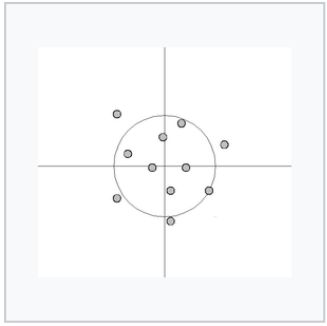

bias low, variance high

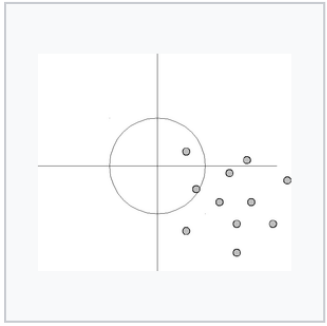

bias high, variance high

# PRad Cross Section Results

W. Xiong *et al.,* Nature **575** (2019) 147–150. https://doi.org/10.1038/s41586-019-1721-2

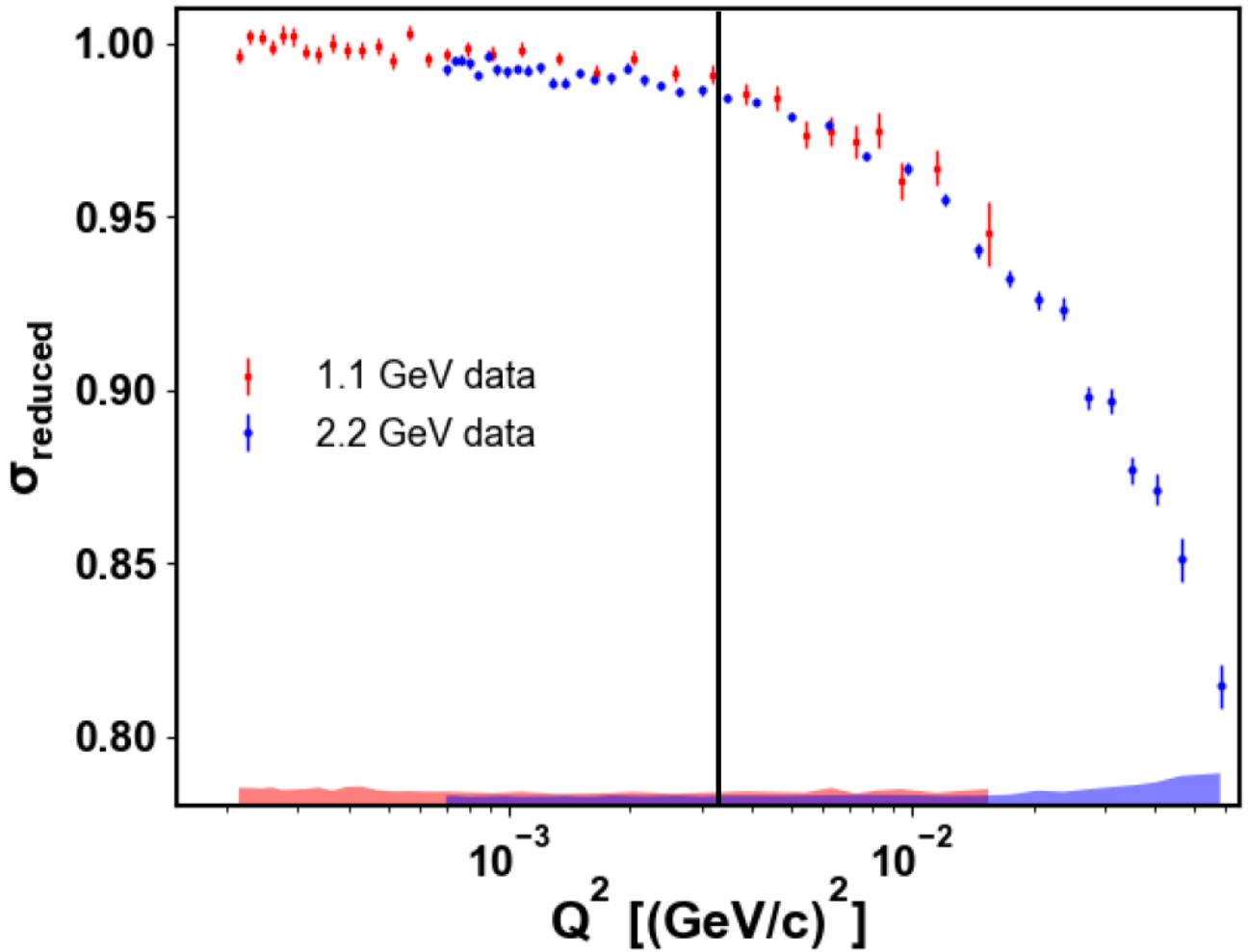


The horizonal line indicates the lowest $Q^2$ point of the Bernauer data of 0.00384 [(GeV/c)$^2$]
The lowest $Q^2$ point of the PRad data is 0.000215 [(GeV/c)$^2$]

# PRad Cross Section Results

W. Xiong *et al.,* Nature **575** (2019) 147–150. https://doi.org/10.1038/s41586-019-1721-2

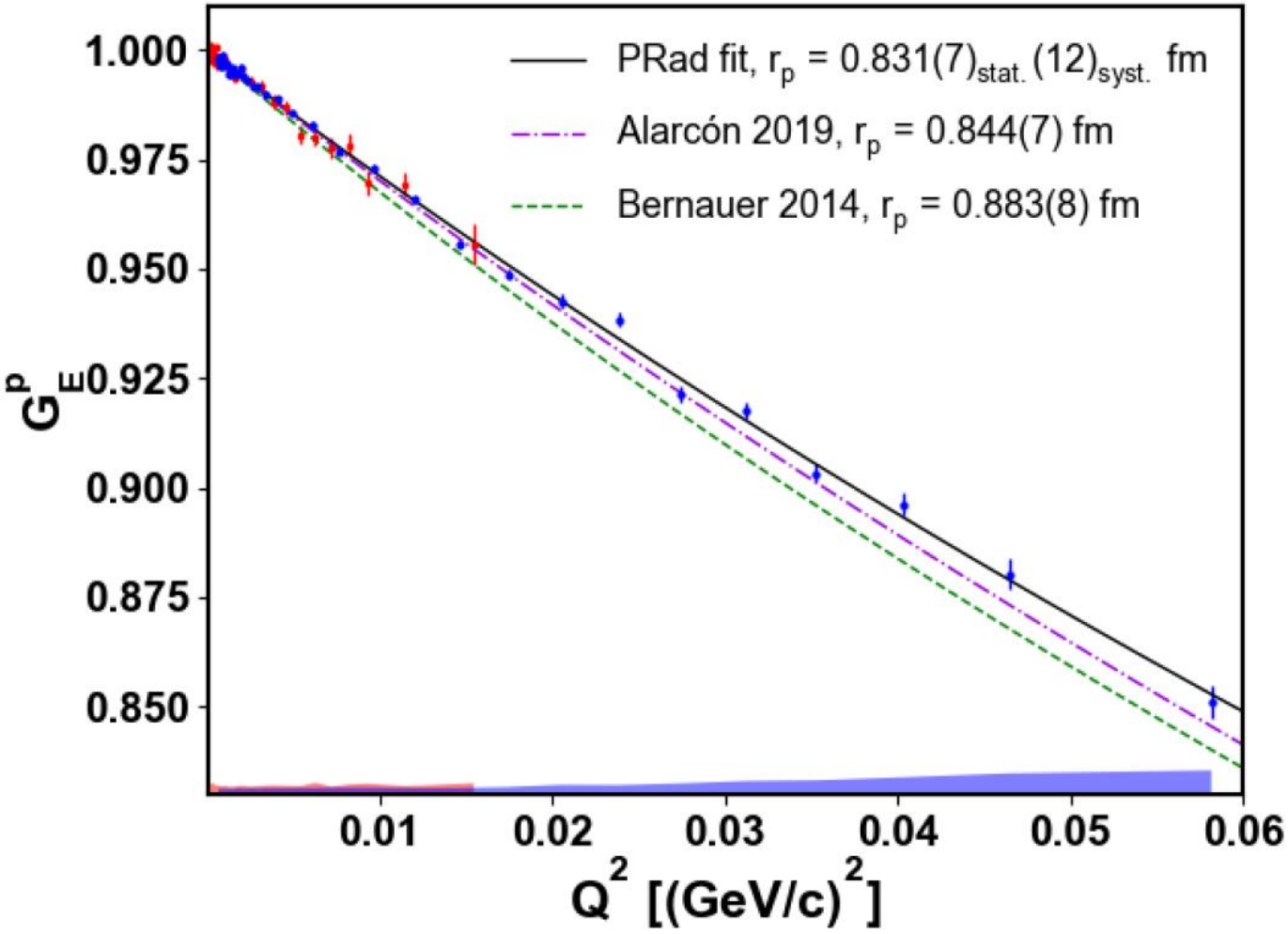

# From Nature Paper Supplemental Material

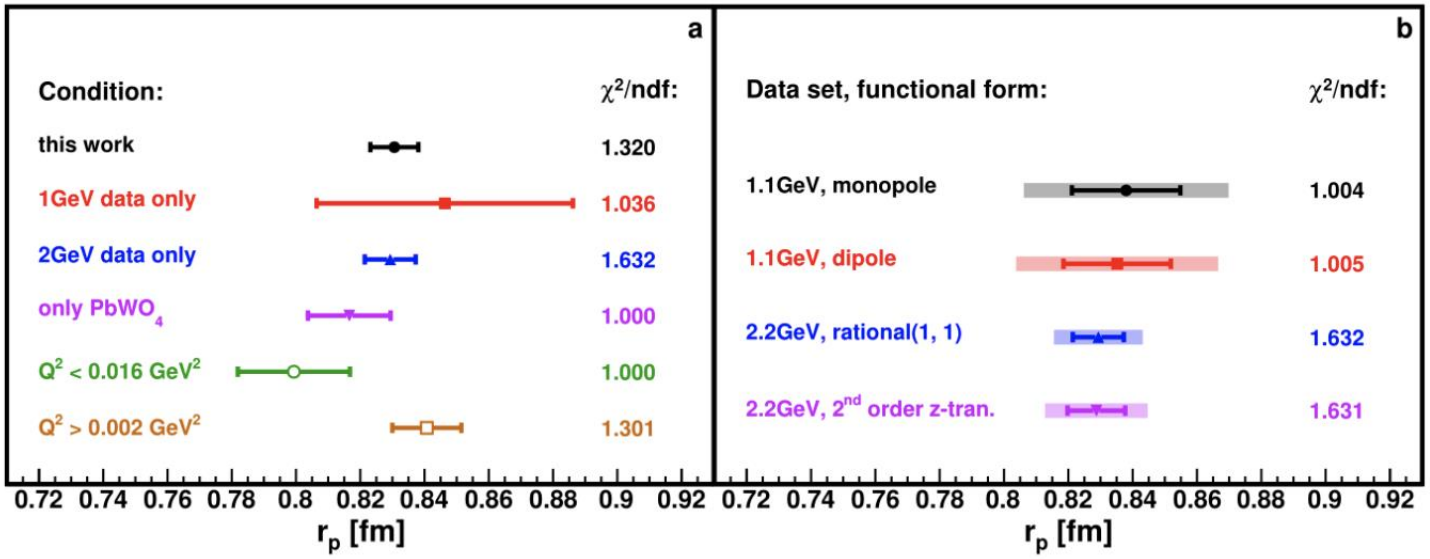


Figure S16: **(a)** The $r_p$ results obtained when using different data sub-sets fit with the Rational (1,1) function. Only the statistical uncertainties are shown here. **(b)** The $r_p$ results obtained when using different data sub-sets but fit with the two best functional forms for these chosen data sub-sets, as determined from the robustness study [17].

# How Analytic Choices Can Affect the Extraction of Electromagnetic Form Factors from Elastic Electron Scattering Cross Section Data

https://doi.org/10.1103/PhysRevC.102.015205
https://arxiv.org/abs/1902.08185

One example in the paper shows, that with all other things fixed, changing the Mainz 1422 data point fit from an unbounded polynomial fit (results shown in light grey) to one where the polynomial parameters are forced to alternate sign (results shown in black) the normalization values to change and the charge radius changes from 0.882 fm to 0.854 fm.

| Energy | Spec. | norm$A$ | norm$B$ | Points | $Q^2$ Range [GeV$^2$] |
|---|---|---|---|---|---|
| 180 MeV | B | $N_1$ | $N_3$ | 106 | 0.0038–0.0129 |
| | B | $N_1$ | $N_4$ | 41 | 0.0101–0.0190 |
| | A | $N_3$ | – | 102 | 0.0112–0.0658 |
| | B | $N_1$ | $N_5$ | 19 | 0.0190–0.0295 |
| | C | $N_2$ | $N_4$ | 38 | 0.0421–0.0740 |
| | C | $N_2$ | $N_5$ | 17 | 0.0740–0.0834 |
| 315 MeV | B | $N_6$ | $N_9$ | 104 | 0.0111–0.0489 |
| | A | $N_7$ | $N_9$ | 38 | 0.0430–0.1391 |
| | A | $N_9$ | – | 40 | 0.0479–0.1441 |
| | C | $N_8$ | $N_9$ | 62 | 0.1128–0.2131 |
| 450 MeV | B | $N_{10}$ | $N_{13}$ | 77 | 0.0152–0.0572 |
| | B | $N_{10}$ | $N_{15}$ | 52 | 0.0572–0.1175 |
| | A | $N_{13}$ | – | 42 | 0.0586–0.2663 |
| | B | $N_{10}$ | $N_{14}$ | 17 | 0.0589–0.0851 |
| | A | $N_{11}$ | $N_{13}$ | 36 | 0.0670–0.2744 |
| | C | $N_{12}$ | $N_{15}$ | 50 | 0.2127–0.3767 |
| | A | $N_{14}$ | – | 2 | 0.2744–0.2744 |
| 585 MeV | B | $N_{16}$ | $N_{18}$ | 41 | 0.0255–0.0433 |
| | B | $N_{16}$ | $N_{19}$ | 47 | 0.0433–0.1110 |
| | A | $N_{18}$ | – | 27 | 0.0590–0.0964 |
| | B | $N_{16}$ | $N_{20}$ | 21 | 0.0920–0.1845 |
| | A | $N_{19}$ | – | 37 | 0.0964–0.4222 |
| | C | $N_{17}$ | $N_{20}$ | 20 | 0.3340–0.5665 |
| 720 MeV | B | $N_{21}$ | $N_{25}$ | 47 | 0.0711–0.1564 |
| | A | $N_{25}$ | – | 46 | 0.1835–0.6761 |
| | C | $N_{24}$ | $N_{26}$ | 28 | 0.6536–0.7603 |
| | B | $N_{23}$ | $N_{26}$ | 27 | 0.2011–0.2520 |
| | C | $N_{22}$ | $N_{26}$ | 37 | 0.4729–0.7474 |
| | B | $N_{21}$ | $N_{26}$ | 36 | 0.1294–0.2435 |
| 855 MeV | B | $N_{27}$ | $N_{31}$ | 35 | 0.3263–0.4378 |
| | C | $N_{28}$ | $N_{31}$ | 31 | 0.7300–0.9772 |
| | A | $N_{29}$ | $N_{30}$ | 32 | 0.3069–0.5011 |
| | A | $N_{29}$ | – | 13 | 0.5274–0.7656 |
| | B | $N_{27}$ | $N_{29}$ | 54 | 0.0868–0.3263 |

$$G_{E,\text{polynomial}}\left(a_i^E, Q^2\right) = 1 + \sum_{i=1}^{n} a_i^E Q^{2\,i} \quad \text{and}$$

$$G_{M,\text{polynomial}}\left(a_i^M, Q^2\right) = \mu_p \left(1 + \sum_{i=1}^{n} a_i^M Q^{2\,i}\right)$$

| | unbound | | bound | |
|---|---|---|---|---|
| i | $a_i^E$ | $a_i^M$ | $a_i^E$ | $a_i^M$ |
| 1 | −3.331 | −2.523 | −3.124 | −2.800 |
| 2 | 13.05 | −0.7081 | 8.821 | 5.188 |
| 3 | −63.68 | 40.16 | −25.74 | −5.742 |
| 4 | 249.4 | −176.7 | 60.06 | 2.806 |
| 5 | −658.6 | 380.3 | −89.41 | −0.000 |
| 6 | 1099 | −392.6 | 72.48 | 0.01034 |
| 7 | −987.6 | 11.53 | −24.23 | −0.2766 |
| 8 | 57.38 | 442.4 | 0.0000 | 0.0000 |
| 9 | 853.4 | −492.1 | −0.0061 | −0.0009 |
| 10 | −810.5 | 230.3 | 0.0081 | 0.0013 |
| 11 | 250.4 | −40.92 | −0.0000 | −0.0000 |

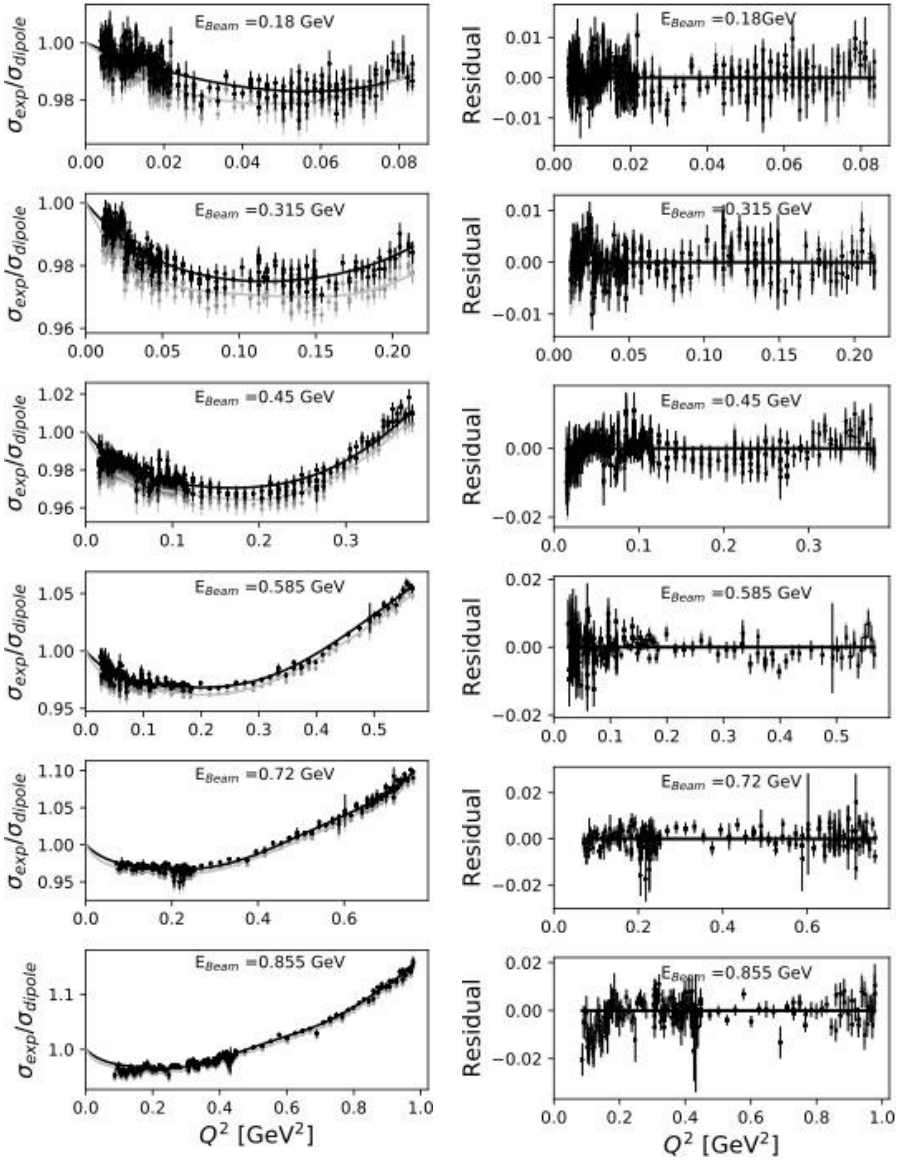

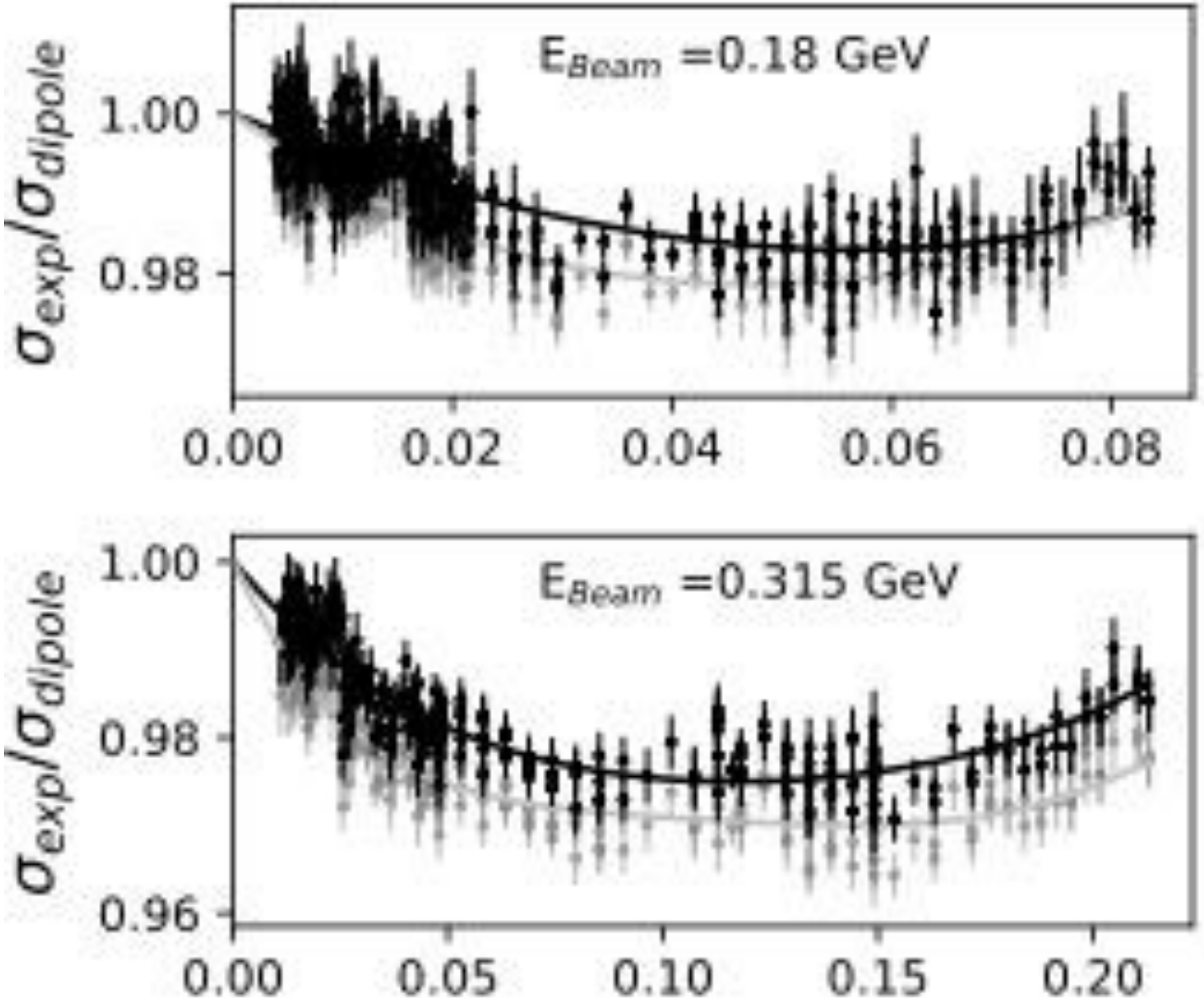
$E_{Beam}$ =0.18 GeV
$\sigma_{exp}/\sigma_{dipole}$
1.00
0.98
0.00
0.02
0.04
0.06
0.08
$E_{Beam}$ =0.315 GeV
$\sigma_{exp}/\sigma_{dipole}$
1.00
0.98
0.96
0.00
0.05
0.10
0.15
0.20
$Q^2$ [(GeV/c)$^2$]

# Comparison of Form Factors

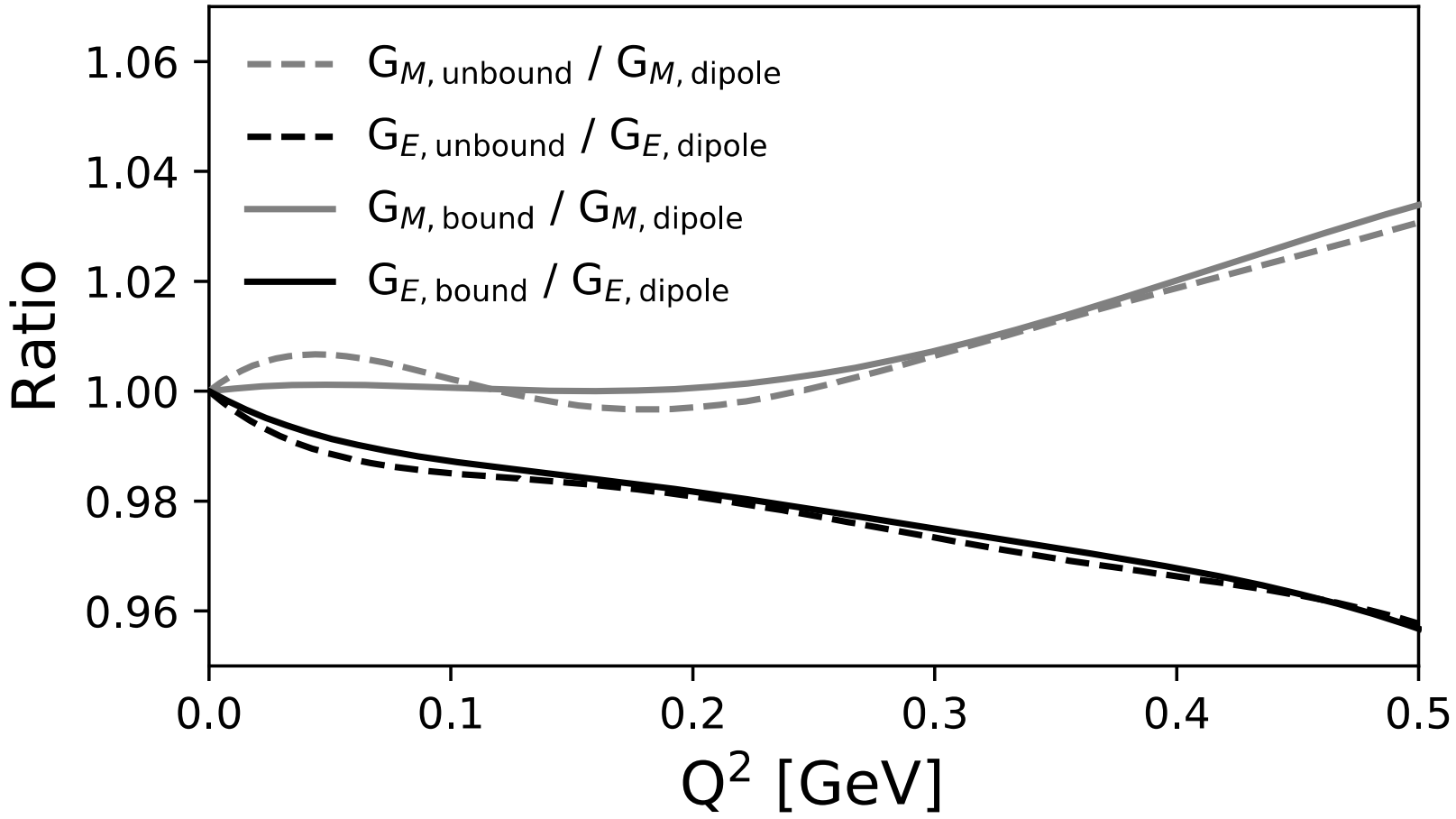


The bounded fit approximates a completely monotone function by alternating signs of terms.
Notice how the bounded fit is smoother then the unbound, but unbounded will always give the lower chi$^2$.
Scott Barcus, DH, Randall E. McClellan, https://doi.org/10.1103/PhysRevC.102.015205

# Comparing PRad and Fit Results

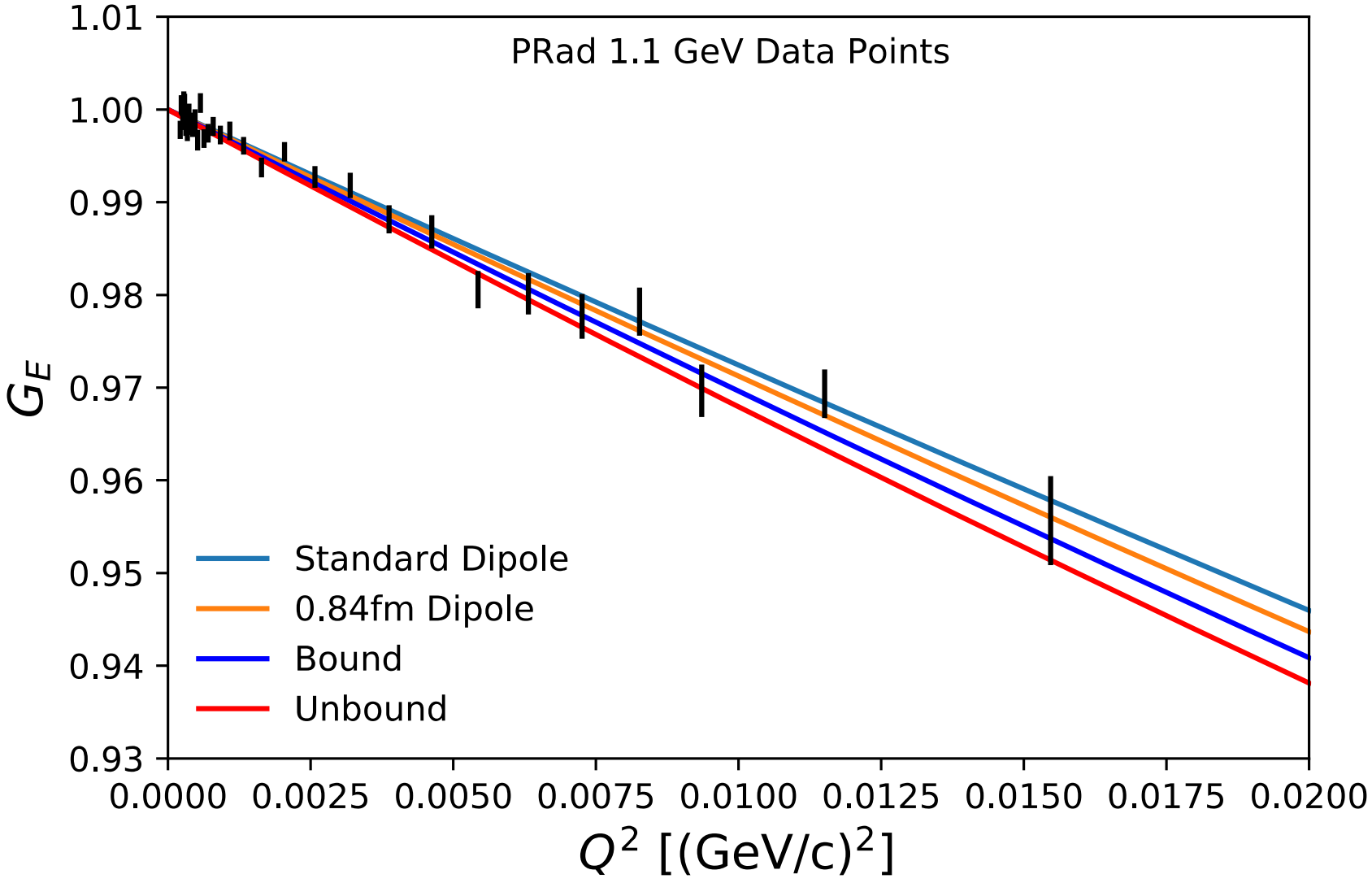

# Comparing PRad and Fit Results

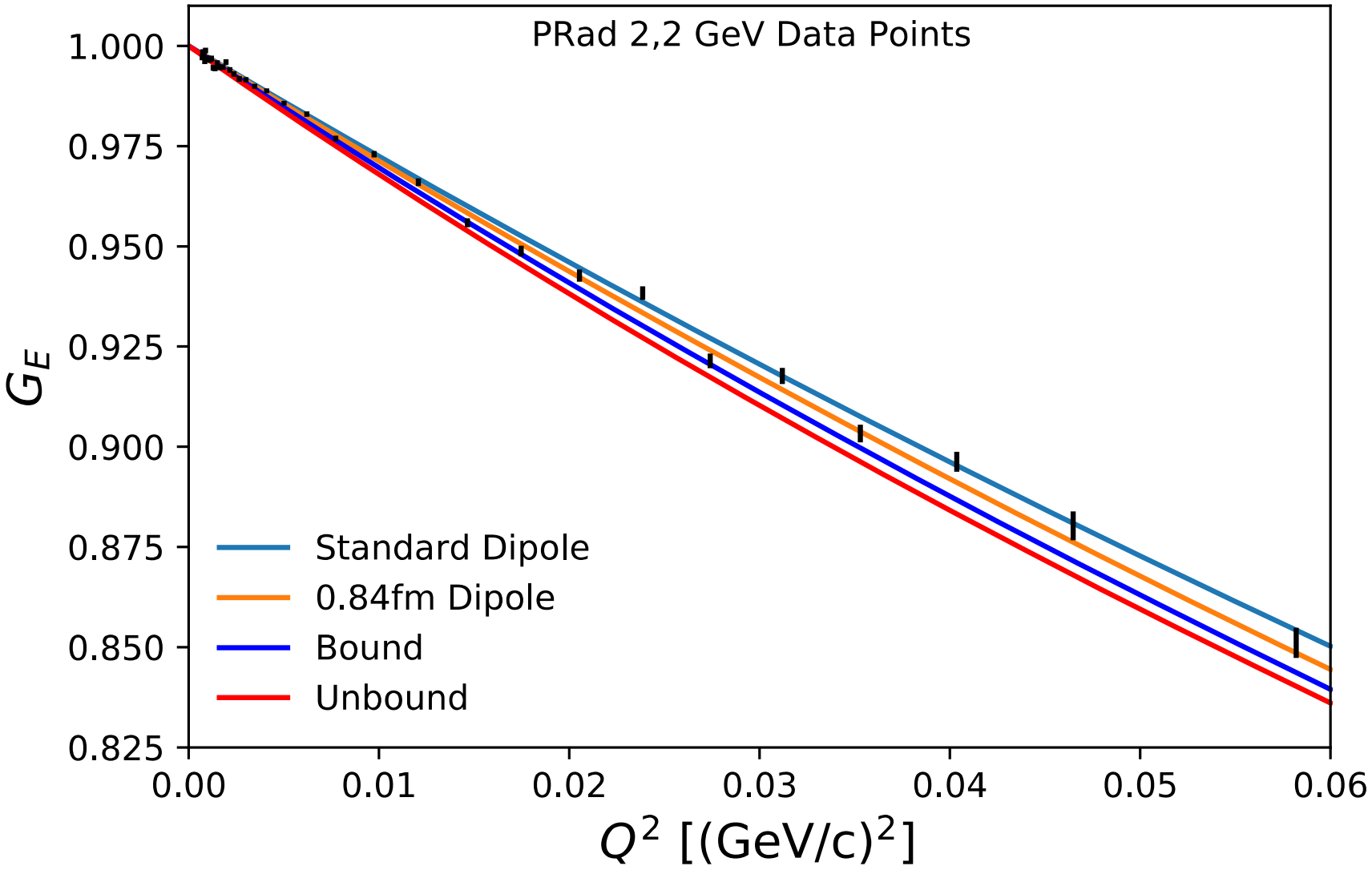


And of course one can fit the sets of data simultaneously.

# Summary and Outlook

- A lot of effort has gone into understanding the proton radius puzzle
  - MANY re-analysis of old and new scattering data
  - PRad (no spectrometer) proton radius 0.831(7) fm
  - New Atomic Lamb shift results mostly consistent with small radius
    - 2020 blinded analysis from Candana was consistent http://doi.org/10.1126/science.aau7807
    - 2017 CRÈME result also consistent with smaller value http://doi.org/10.1126/science.aah6677
    - But 2018 French result still gives previous value https://doi.org/10.1103/PhysRevLett.120.183001
  - **MUSE, New Mainz A1 Data, MESA, Compass, PRAD-II and more still to come**
- From Hohler in 1976 to the Dispersively Improved Chiral Effective Field Theory of Alarcon and Weiss in 2022, conventional nuclear theory seems consistent with a smaller radius, thus it would seem the larger radius is the one that would point to new physics.
- As was shown in the analytic choice paper, in complex regressions, small changes can have large impact on the results.

# **VERY TENATIVE** LONG TERM SCHEDULE FOR JEFFERSON Lab

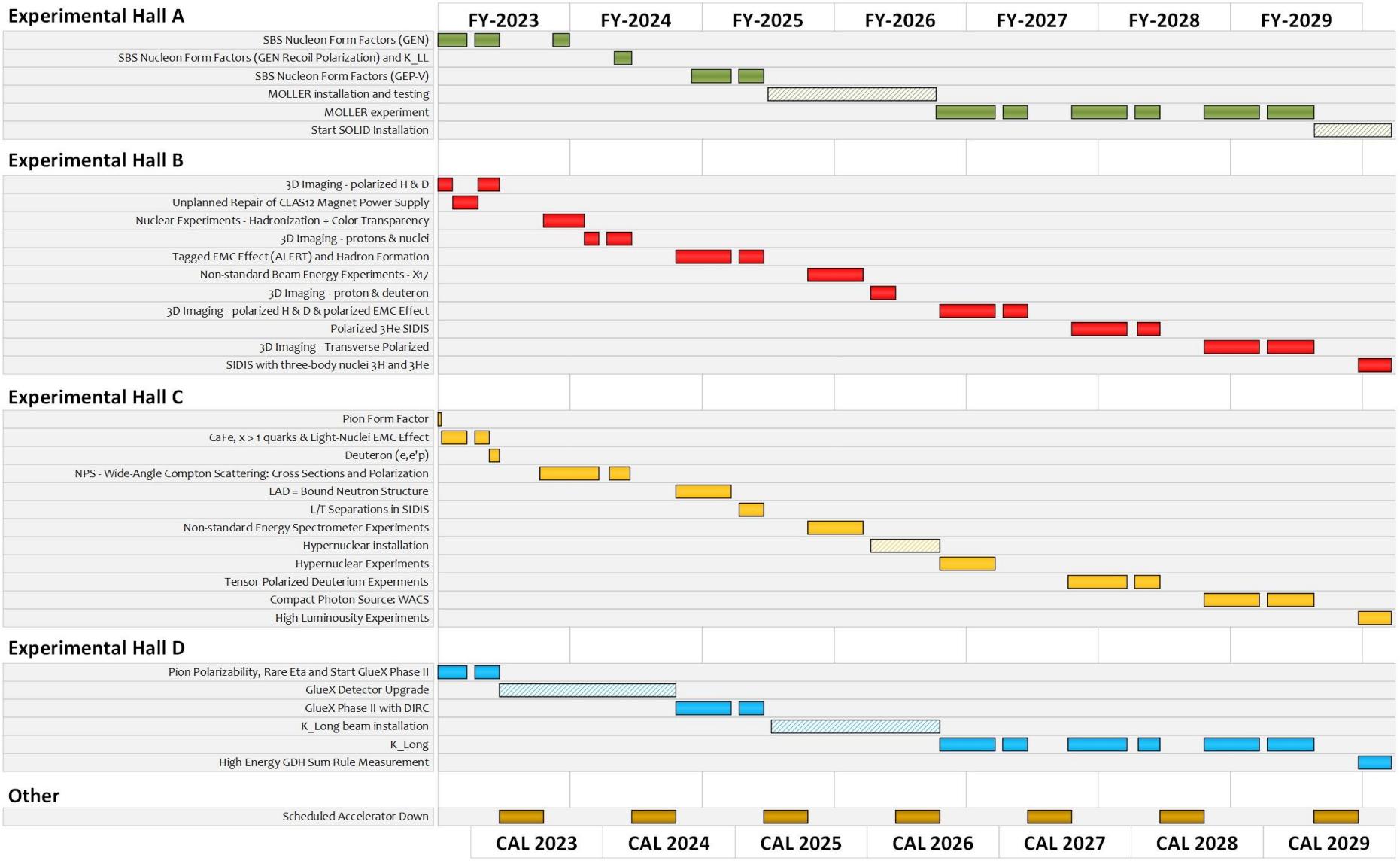

# Robust Regressions

https://doi.org/10.1103/PhysRevC.102.015205

- Ordinary Least Squares Regressions are easily "pulled" by a single point.
- Robust regressions tend to follow the global trends.

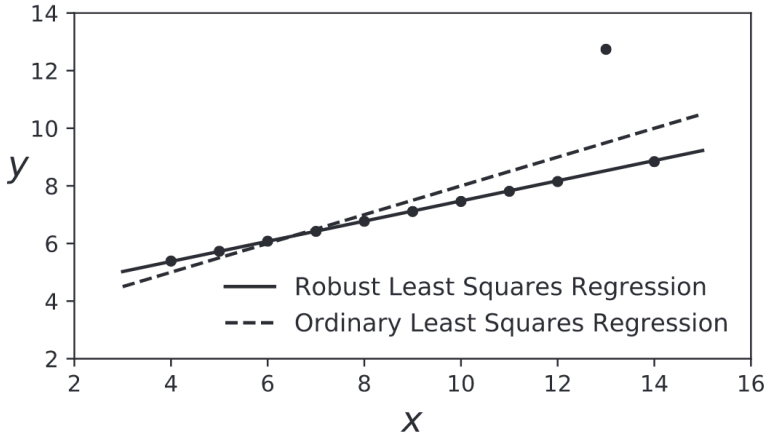


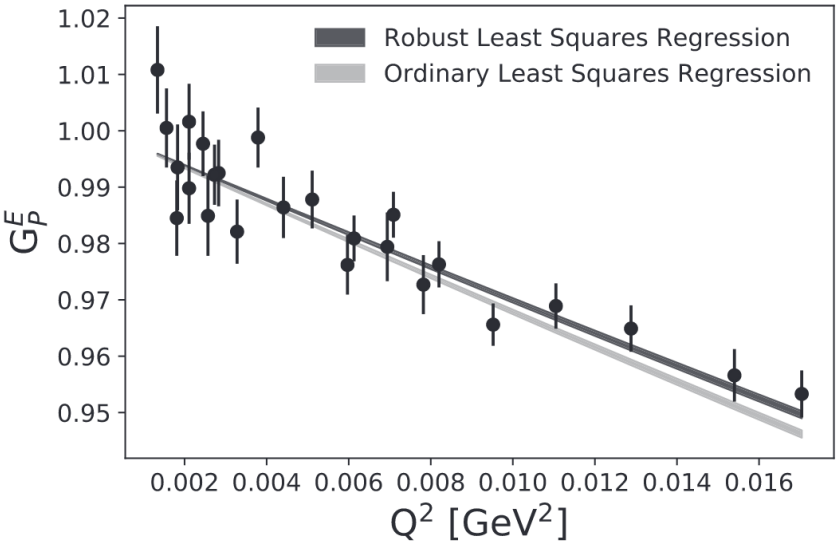


FIG. 8. Proton electric form factor data taken from the ISR dataset found in the Supplemental Material of Ref. [57]. The uncertainties are calculated by summing the listed statistical uncertainties with the systematic uncorrelated uncertainties in quadrature. The theoretical model used for the regressions is the model of Alarcón and Weiss [24], with only one free parameter. These regressions give a proton radius of 0.874 fm for the OLSR and 0.844 fm for the RLSR with soft loss.

https://doi.org/10.1103/PhysRevC.102.015205

Many functions can be used for $\rho(z)$ to introduce robustness, but for the following examples the 'soft loss' (softl1) function given in Eq. A3 was selected and implemented using the Python package SciPy [54–56].

$$\chi^2 \equiv \sum_{i=1}^{N} \rho_i(z) \text{ and } z = \left( \frac{y_i - y(x_i | a_1, a_2, ..., a_M)}{\sigma_i} \right)^2$$

$$\rho(z) = 2\left(\sqrt{1+z} - 1\right)$$

With soft loss, as a $z_i$ gets larger, the magnitude of $\rho_i(z)$ is increasingly reduced with respect to OLSR. A RLSR with soft loss essentially re-weights the outliers of a dataset, decreasing their influence when fitting. Note that if a dataset meets all of the above assumptions inherent to OLSR (i.e. errors are normally distributed, uncorrelated, and have the same variance) then OLSR and RLSR techniques should both produce the same fit results since the dataset, by definition, does not contain excessive outliers.